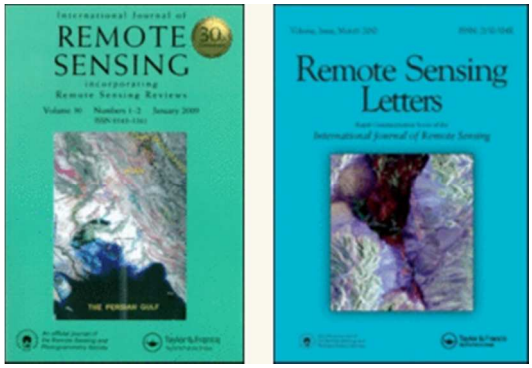

Adaptive retracking of Jason-1 altimetry data for inland waters on the example of the Gorky Reservoir

Journal:	*International Journal of Remote Sensing*
Manuscript ID:	TRES-SIP-2010-0073.R1
Manuscript Type:	IJRS Special Issue Paper
Date Submitted by the Author:	n/a
Complete List of Authors:	Troitskaya, Yuliya; Institute of Applied Physics Rybushkina, Galina; Institute of Applied Physics Soustova, Irina; Institute of Applied Physics Balandina, Galina; Institute of Applied Physics Lebedev, Sergey; Geophysical Center of RAS Kostyanoy, Andrey; P.P. Shirshov Institute of Oceanology RAS
Keywords:	COASTAL, ALTIMETRY
Keywords (user defined):	Inland , water, bodies

Adaptive retracking of Jason-1 altimetry data for inland waters on the example of the Gorky Reservoir

Yu. Troitskaya [ab], G. Rybushkina [a], I. Soustova [a], G. Balandina [a], S. Lebedev [cd], and A. Kostianoy [e]

[a] Institute of Applied Physics RAS, Nizhny Novgorod, Russia – ryb@appl.sci-nnov.ru
[b] Obukhov Institute of Atmospheric Physics RAS, Russia
[c] Geophysical Center of RAS, Moscow, Russia – s.lebedev@gcras.ru
[d] Space Research Institute RAS, Russia
[e] P.P. Shirshov Institute of Oceanology RAS – kostianoy@Óhean.ru

Abstract – Standard altimetry data processing developed for the open ocean conditions can be inapplicable for the case of inland waters, especially ~~in~~ for narrow elongated water bodies and rivers, where the distance between shores is less than 5-10 km (while the eliminated area within the gain of the radar antenna for Jason-1,2 is about 50 km). These conditions are typical, for example, for the majority of reservoirs of the Volga river cascade (with one exception, Rybinskoe Reservoir). Under these conditions only a few telemetric impulses fit the validity criteria, which causes a severe loss of data. Besides, errors in the water level retrieved from the altimetric measurements are enormous, as it was demonstrated on the basis of comparison of in situ measurements at hydro gauging stations for the water level of Gorky Reservoir of the Volga River and all available along track 10Hz TOPEX / Poseidon altimetry data and 20Hz Jason altimetry data over the reservoir area.

The problem of minimization of the errors can be resolved by retracking. For justification of the optimal retracking algorithm the average impulse response of the statistically inhomogeneous surface were calculated theoretically based on the works of Brown, 1977 and Barrick and Lipa, 1985 for the model of the terrain in the vicinity of Gorky Reservoir. The model represents the main typical features of the waveform examples (e.g., high peaks or irregular complex shape), the modeled waveforms are in good agreement with the Jason-1,2 waveforms for the same area. It was shown, that for Gorky Reservoir significant wave height (SWH) did not exceed 0.5 m (corresponding to the width of the leading edge less than 1 telemetric gate). Under these conditions the retracking algorithm based on the detection of the beginning of the leading edge of telemetric impulses is preferable for correct assessment of variations of water level in Gorky Reservoir.

Comparing with the data of in situ measurements at hydro gauging stations for the water level of Gorky Reservoir shows that retracking dramatically increases the number of data involved in monitoring and significantly improves measurements of the water level. Validation of retracked data of water level by comparison Jason-2 and Jason-1 after maneuver measurements for Gorky Reservoir is also carried out. General principals of retracking algorithms for complex area (land, coastal zone, inland waters, etc) based on calculations of the waveform taking into account statistical inhomogeneity of the reflecting surface adjusted to a certain geographic region are discussed.

Keywords: coastal altimetry, inland water bodies

1. INTRODUCTION

Altimetry data processing algorithms developed for the open ocean may be inapplicable for the case of coastal and inland waters. The problems of inland water data processing are very similar to those arising in the coastal zone of the ocean from contamination of the received signal by reflection from the land. This effect is very strong in the Gorky Reservoir with the maximum width of 14 km and steep 10-20 m banks. Under these conditions few telemetric pulses fit the validity criterion, which causes severe data loss. As a result, the Gorky Reservoir is not included in the data bases by LEGOS and the U.S. Department of Agriculture's Foreign Agricultural Service. This work is about the experience of retrieving the water level in the Gorky Reservoir by an adaptive retracking algorithm, which dramatically increases the number of data involved in monitoring. General principles of the considered regional retracking algorithm may be useful for altimetry of another cases of inland water bodies and coastal zones.

2. FEATURES OF INLAND WATER ALTIMERTRY. FUNDAMENTALS OF THE METHOD OF ADAPTIVE REGIONAL RETRACKING

In the coastal zone, altimeter waveforms differ significantly from those formed in the open ocean. This occurs due to the impact of land reflection. Figure 1 shows examples of telemetric waveforms generated by reflection from land and water (fig. 1a), quasi-specular coherent reflection from a smooth water surface in estuaries and harbors (fig. 1b), and other highly reflective objects (coastal buildings, large slick areas, etc.), see fig. 1c.

In the presence of additional peaks the waveform is poorly approximated by Brown's formula [Brown 1977], which leads to error in determining the position of the leading edge and, hence, to wrong determination of satellite altitude and water level, when the Brown-like formula based algorithms are applied. In this case, the other quantities, such as wind speed and significant wave height (SWH) are also determined incorrectly. In this regard, recently special algorithms have been actively developed for re-processing altimetry data in the coastal zone [Anzenhofer et al. 1999, Deng and Featherstone 2006], large rivers[Koblinsky et al. 1993, Birkett 1998, Alsdorf et al. 2001, Benveniste&Berry 2004, Berry 2005, Frappart et al. 2005,2006] and lakes [Birkett 1995, Kostyanoi et al. 2004, Cretaux et al. 2010] . But there is still no standard technique which would allow using a satellite data base for correct assessment of water level in the conditions, when the reflection from land strongly affects the received waveforms. There exist various retracking algorithms for determining the leading edge arrival time of the reflected signal, for example, threshold retracking, β-retracking [Martin 1983, Davis 1997, Deng and Featherstone 2006, Lee 2008], etc. In this paper, we propose a method of regional adaptive retracking based on constructing a theoretical model describing the formation of telemetric waveforms by reflection from the piecewise constant model surface (fig. 2) corresponding to the geography of the region. On this basis we formulate the criteria for selecting the telemetric waveforms and justify the applicability of the threshold and the improved threshold retracking algorithm for determining the parameters of the underlying surface in inland water basins. Possible applications of these methods to the Gorky Reservoir on the Volga River are also considered.

For the open ocean conditions the algorithm for determining the parameters of the underlying surface is based on the approximation of the altimeter waveform by the well-known Brown's formula [Brown 1977] , derivation of which is based on the model of incoherent scattering of radio waves by a rough surface. Assuming that the radio waves

coming from different parts of the surface are added incoherently, the power of the reflected signal is given by [Brown 1977, Barrick&Lipa 1985]:

$$P(t) = P_0 \iint\limits_{\substack{illu\min ated \\ area}} \frac{G^2(\theta)\sigma(x,y,\theta)}{r^4} dA \int_{-\infty}^{\infty} p\left(t_1 - \frac{2r}{c}\right) q\left(x, y, \frac{c}{2}(t-t_1)\right) dt_1, \quad (1.1)$$

where G is the gain of the radar antenna, r is the distance from the radar to the elementary scattering area dA on the surface, x,y- cartesian coordinates on the surface, θ - is the angle, measured from antenna boresight axis to the area dA direction (see fig. 3), σ is the backscattering cross-section per unit scattering area, $p(t)$ is the radar system point-target response and q(z) is the height probability density of specular points.

The transformations made in [Brown 1977] for the case of small-angle approximation, small deviation of altimeter antenna axis from nadir ($\theta << 1$ and $\xi << 1$, see fig. 3), and model expressions for G, q, p, σ:

$$\begin{gathered} \mathrm{G}(\theta) = \exp(-2\sin^2\theta/\gamma), \quad q(z) = \frac{1}{s\sqrt{2\pi}}\exp(-z^2/2s^2), \\ p(t) = \frac{1}{\tau_i\sqrt{2\pi}}\exp(-t^2/2\tau_i^2), \quad \sigma = \sigma^{(0)} \cdot e^{-\alpha\, tg^2\theta} \end{gathered} \quad (1.2)$$

give the following expression for the waveform reflected from an infinite statistically homogeneous underlying surface:

$$\begin{gathered} P\left(t - \frac{2h}{c}\right) = \frac{P_0\sigma^{(0)}}{2h^4}\left(1 + \mathrm{erf}\left(\frac{(ct-2h)}{\sqrt{2}\sqrt{(2s)^2 + c^2\tau_i^2}}\right)\right) \times \\ \times \exp\left[-\frac{4}{\gamma}\sin^2\xi - \frac{c}{h}\left(t - \frac{2h}{c}\right)\left(\frac{4}{\gamma}\cos 2\xi + \alpha\right)\right] I_0\left(\frac{4}{\gamma}\sin 2\xi\sqrt{\frac{c}{h}\left(t - \frac{2h}{c}\right)}\right), \end{gathered} \quad (1.3)$$

where h is the mean distance from the satellite to the underlying surface. In the case of an inland water body the altimeter footprint consists of several parts differing in heights and reflecting properties (e.g., water, swamp, dry land, etc). They are schematically shown by different shading in fig. 2. If we assume that the altimeter antenna axis is aimed strictly at nadir, then contribution of each part to the reflection is described by the analogue of Brown's formula (see (1.3) for $\xi = 0$), which is multiplied by $\Delta\varphi_k/2\pi$ to take into account the contribution of k-th area:

$$P_k(\tau) = \frac{P_0\sigma_k^{(0)}}{4\pi h^4} e^{-\left(\frac{4}{\gamma}+\alpha_k\right)\frac{(c\tau - 2H_k)}{h}} \left(1 + \mathrm{erf}\left(\frac{(c\tau - 2H_k)}{\sqrt{2}\sqrt{(2s_k)^2 + c^2\tau_i^2}}\right)\right) \times \Delta\varphi_k. \quad (1.4)$$

Here parameters with index k: $H_k, \sigma_k^{(0)}, \alpha_k, s_k$ correspond to the level, scattering properties and roughness for a given (k-th) part of the underlying surface (H_k is positive when the distance from the surface to the satellite is greater than the mean value and the surface level is lower than the mean value). In (1.4) we take into account the fact that at time $\tau = t - 2h/c$

the main contribution to the reflection from k-th illuminated area is given by an arc $\Delta\varphi_k$ (see fig. 2) centered at the nadir point with coordinates x_N, y_N and determined by the condition of equality of the distance from the antenna to *k-th* piece of surface. The radius of the arc is equal to $\sqrt{h\left(c\tau - 2H_k\right)}$ and depends on the deviation of the surface level of this area from the average value. If the surfaces have different elevations, the beam will contact them at different angles; it is schematically illustrated by fig 2b.

The total reflected power is the sum of contributions from all piecewise constant regions:

$$P(\tau) = \sum_{k=1}^{3} P_k(\tau) \qquad (1.5)$$

Using (1.4) and (1.5) one can calculate the reflected waveforms and their change when the satellite moves along the track.

3. AN EXAMPLE OF USING THE ADAPTIVE REGIONAL RETRACKING METHOD FOR DETERMINING THE WATER LEVEL IN THE GORKY RESERVOIR

3.1 Problems arising in determining the water level in the Gorky Reservoir by data from GDR base of Jason-1 satellite

According to NASA/CNES data (see fig. 4) the water area of the Gorky Reservoir and the Volga River is intersected by 2 groundtracks (pass 33 and pass 142) of altimetry satellites T/P and Jason-1,2 and several tracks of altimetry satellites ERS-1, ERS-2, ENVISAT, GEOSAT, and GFO.

We used data for the 142-nd pass of Jason-1 (before maneuver), which intersects the Gorky Reservoir in its northern part (fig. 1), with the track length within the reservoir being about 15 km. The altimetry data of this track were compared with the measurements from the ground station in Yurievets (a small town on the right bank of the Gorky Reservoir). At the first stage, Geophysical Data Records (GDR) of Jason-1 (J1) satellite were processed. All altimetry 20Hz Jason-1 data available along the pass 142 were used and all available in the original altimetric data bases corrections were calculated [AVISO 1996, Picot et al. 2008]. The "wet" and "dry" troposphere corrections were calculated by meteorological data (atmospheric pressure and air humidity) from the nearest weather station. DORIS ionosphere correction was used for correcting altimetry measurements of reservoir surface height. The sea state bias correction was determined on the basis of model calculations. All the corrections are. Corrections for the state of the underlying surface, "inverse barometer" and oceanic and pole tides that are used for determining oceanic levels need not be taken into consideration for inland waters. A similar procedure had been used earlier for determining the hydrological regime of large rivers in South America, Africa and Siberia - see, e.g., Campos et al. (2001), Birkett et al. (2002), Maneu et al. (2003), Kouraev et al. (2004), as well as for assessing the water level in the lower reaches of the Volga river [Lebedev & Kostyanoi 2005]. Comparison with data of hydro gauging stations verified efficiency of this procedure for large inland water areas.

Results of the data processing following the described procedure were used to plot water levels in the Gorky Reservoir with a resolution of 10 days in the period from 2002 to 2007 (grey squares in fig. 5a). The results were compared with the measurement data obtained at the hydro gauging stations of the State observation network (solid line in fig. 5a). The correlation coefficient of altimetry data and in situ measurements is about 0.33 (fig. 5b). Low correlation of satellite and ground-based measurements is explained by significant loss of data

and large errors caused by the shortcomings of direct application of the altimetry algorithms for water level retrieving designed for large water areas (oceans and seas) to middle size water basins, in which the footprint of radio-altimeter largely falls on the land.

To clarify the causes of significant errors we analyzed the waveforms of the reflected pulses received by the altimetry antenna. The needed data were taken from the SGDR data base of Jason-1 satellite. Special software was developed for analysis of averaged reflected waveforms for high spatial resolution points with the averaging interval of 0.05 s. The software enables tracing changes in the waveform as the nadir point is moving along the satellite track. Examples of varying waveforms for a point moving in the area marked by the white circle in the map are presented in fig. 6.

The waveforms shown in the lower figure on the left represent the received reflected power as a function of time (the number of altimeter gate is laid off along the horizontal axis, 1 gate corresponds to the time interval dtg=3.125 ns; and the power of the reflected signal is laid off along the vertical axis). Analysis of these waveforms suggests that the scatter in the water level data may be caused by drawbacks of the standard algorithm of computations in which the 32-nd gate of the plots is regarded to be the arrival time of the reflected signal. However, one can see from the plot presented above that the reflected signal may also arrive both before and after the mentioned gate, whereas the error of 1 gate leads to the error in water level measurements of $dtg*c_{light}/2 \approx 50$ cm.

Besides, the hydrometeorological regime of the Gorky Reservoir has strong seasonal variability. In winter lasting from November to April the entire water area is covered by ice and a snow layer, while the average date of freezing is November 22 (usually between November 7 and December 7) and average date of clearing from ice of the lake part of the reservoir is May 3 (usually between April 18 and May 18). The summer season when the water area is free of ice lasts from May to October. Examples of Jason-1 Ku-band waveforms for winter and summer seasons are given in fig. 7.

In winter (fig. 7a) the waveforms are more or less regular and are fit for ice retracking. The summer waveforms (fig. 7b) are complex, they can have quasi-specula or multiple quasi-specula components, etc. Brown's (1977) formula is not typically valid for approximation of such waveforms and an adaptive retracking algorithm is required.

3.2. Piecewise constant model of telemetric pulse scattering for the Gorky Reservoir and its neighbourhood

For calculation of telemetric waveforms within the framework of model (1.4), (1.5) the underlying surface near the 142-nd track of Jason-1 and T/P satellites (fig. 8a) was approximated by the piecewise model depicted in fig. 8b, where water and land are shown by different shading. Note that our field studies revealed the specific feature of the Gorky Reservoir water area that could significantly influence the reflected waveforms. Smoothed regions 20-30 m wide (light-grey stripes in fig. 8b) were regularly observed near the coastline, which were evidently caused by high concentrations of surface active substances associated with economic activity. Such smoothed regions are known to give rise to peaks in telemetric pulses[Tournadre et al. 2006] .

For analysis of the contribution of slicks let us transform the expression (1.1) with allowance for the simplifying assumptions adopted in Sec. 1. Then, (1.1) takes on the form

$$P_i(\tau) = \frac{P_0}{\sqrt{2\pi h^4}} \iint \frac{\sigma^{(0)}}{\sqrt{(2s)^2 + c^2\tau_i^2}} e^{-\left(\frac{4}{\gamma}+\alpha\right)\frac{\rho^2}{h^2}} e^{-\frac{\left(c\tau - 2H - \rho^2/h\right)^2}{\left(8s^2 + 2c^2\tau_i^2\right)}} dA \qquad (1.6)$$

In this expression parameters of the surface are functions of coordinates, $\rho^2 = (x - x_N)^2 + (y - y_N)^2$, x_N, y_N are the coordinates of a nadir point. Note, that the slick water surface is almost smooth, so $\sqrt{8s^2 + 2c^2\tau_i^2} \approx \sqrt{2}\, c\tau_i$. For sufficiently short probe pulses, when the inequality $\left(\frac{4}{\gamma} + \alpha\right)\frac{\sqrt{2}c\tau_i}{h} << 1$ is valid, the second exponential in (1.6) represents a peak function with the maximum at $c\tau - 2H = \rho^2 / h$, which enable one to take the other factors outside the integral by setting them equal to the value at this point. Taking this into attention, we can simplify this expression, then for narrow slicks extending along the coastline (coastal slicks) we obtain

$$P_{sl}(\tau) = \frac{P_0 \sigma_{sl}^{(0)} d_{sl}}{\sqrt{2\pi} h^4 c\tau_i} e^{-\left(\frac{4}{\gamma}+\alpha_{sl}\right)\frac{c\tau - 2H_{water}}{h}} \int_C e^{\left\{-\left(c\tau - 2H_{water} - \frac{(x(l)-x_N)^2 + (y(l)-y_N)^2}{h}\right)^2 \Big/ 2c^2\tau^2{}_i\right\}} dl, \quad (1.7)$$

where $y=y(l)$, $x=x(l)$ is the equation of the coastal line C, and d_{sl} is the width of the slick.

The reflected power received by the altimeter's antenna is the sum of the contributions from water and land described by (1.4) and the contribution of coastal slicks (1.7):

$$P(\tau) = P_{water}(\tau) + P_{land}(\tau) + P_{sl}(\tau) \quad (1.8)$$

Parameters in formulas (1.4), (1.7) are determined by the properties of the reflecting surface. For the water surface: elevation H is the water level, s is a significant wave height and σ is determined by the wind speed. For the land surface, H is determined by topography, s is surface roughness, σ is determined by the reflecting properties of the land. The model was constructed assuming that parameters of land are fixed, and the characteristics of surface water (water level, wave height and roughness) are variable and must be determined using the retracking algorithm.

For the case of underlying surface in the vicinity of the 142-nd Jason-1 pass we suggested a simplified piecewise constant geographical model of reflecting surface for Gorky reservoir (compare fig.8a and fig.8b). The main simplification concerned the model of the land, which was supposed to have a constant height H=20m (an average height of the area according to Global Land One-km Base Elevation Project [GLOBE], see fig.9). The shorelines were modelled by strait lines: $y=0$ for $x<0$, $x=0$ for $y<0$, $y = 0.25\,x + 5400$ for $-21600 < x < 14240$, $y = 4\,x - 48000$ for $0 < x < 14240$.

Then, based on formulas (1.4), (1.7) and (1.8) the reflected waveforms for the 142-nd Jason-1 track were calculated. The arcs $\Delta\varphi_k$ in (1.4) were calculated numerically for different times as the satellite moves along the track.

The contributions of water surface reflections to the telemetric waveforms were modelled assuming that the water level was spatially homogeneous over the reservoir. For determining parameter s one needs to know the significant wind wave height found from data on the wind speed and direction measured at the Yurievets weather station (57°20'N 43°07'E) fig. 10a,b. It is worth noting that the wind speed in the reservoir water area does not coincide with the wind speed measured at the coastal weather station in Yurievets. Special in-situ measurements showed that wind speed in the water area is 1.5-2 times that on the coast.

The SWH was estimated from the empirical relation obtained by generalizing the measurements on Lake Ontario [Donelan et al. 1985]:

$$SWH = 0.2074 \frac{U_{10}^2}{g} \Omega^{-1.55}, \quad (1.9)$$

where $\Omega = U_{10}/c_p$ is the parameter characterizing wave height age, U_{10} is the wind speed at the height of 10 m, and c_p is the phase velocity of wind-wave spectral peak. Donelan [Donelan et al. 1985] showed that Ω is related to fetch x by the empirical formula

$$\Omega = 22\left(\frac{gx}{U_{10}^2}\right)^{-0.33} \tag{1.10}$$

For estimation of the statistics of surface waves we calculated angular distribution of fetches as a function of wind direction for the average point of the 142-nd track of the altimetry satellites in the reservoir water area. The reservoir is anisotropic because of its elongated shape and maximum fetch is attained with south-southwest wind (fig. 10 c).

Using histograms of wind speed distribution obtained at the Yurievets weather station taking into consideration the coefficient of the speed of wind from land to the reservoir water area, as well as histograms of the angular fetch distribution we calculated statistics of the significant wave heights in the Gorky Reservoir in the summer period by formulas (1.9) and (1.10). The histogram of wave height distribution is presented in fig. 10d. Calculation of the statistical expectation shows that average wave height in the Gorky Reservoir in the summer period is very small, about 0.28 m.

Reflective properties of land, water and slicks are not exactly known for the region considered. However, taking into account that the ratio of the reflection coefficients rather than their absolute values are important for the construction of waveforms, we choose the coefficients from physical considerations: for land $\sigma^{(0)} = 20, \alpha = 10$, for water $\sigma^{(0)} = 50, \alpha = 10$, for coast slicks $\sigma^{(0)} d_{sl} = 0.5, \alpha = 1000$. The parameters specific to the radar altimeter were set equal to $\gamma = 0.0005, \tau_i = 0.425T$, where $T = 3.125 \cdot 10^{-9} s$ - the point target response 3 dB width.

Choosing parameters of the model (1.4), (1.7) and (1.8) in conformity with the above estimates we calculated waveforms of telemetric pulses. Our calculations correspond to the summer period. The winter case requires special consideration, since the conditions are quite different. In winter the water is covered with ice and snow, and the land is also covered with snow, whose thickness can reach 1-2 m. As a result the waveforms from the area considered are more similar to the ocean ones (see fig. 7a).

The calculated summer model waveforms reflected from the surface close to the Gorky Reservoir are shown in fig. 11. The results are presented in fig. 11 b as a histogram of telemetric waveforms (the coordinates are: time – distance along the track). Time is measured in units of telemetry gate (3.125 ns), and distance in terms of counts along the track (700 m). The complex form of the images reflects the complexity of the calculated model waveforms. Their characteristic features are parabolic singularities corresponding to the reflection from the coast and scattered on the slicks near the coast. By virtue of the small value of the average SWH (28 cm) the waveforms have an extremely narrow leading edge corresponding to less than 1 telemetry gate.

Based on these peculiarities of the calculated waveforms we set the validity criteria for waveforms in the regional retracking algorithm:

1) to determine the water level one should take the waveforms from the 43.14 - 43.22 E section of the Gorky Reservoir (the lower half of the chart in fig. 11b corresponding to the region between the marks in fig. 11 a), because only in this region we can reliably distinguish the signal reflected from water: the leading edge of this pulse falls on the 32-nd remote gate, where it was placed purposefully in the calculations in accordance with signal processing on the satellite (the model reflected power arriving before the 32-nd gate is connected with reflection from higher parts of the surface);

2) the deviation of the water level from an average value by more than 2 m should be considered erroneous.

For the valid waveforms we propose the following regional retracking algorithms appropriate for the Gorky Reservoir for track 142, including 2 steps. At the first step we estimate a tracking point determined by a definite threshold. The second step is refinement of the estimates: 4 points in the neighbourhood of the threshold (fig. 12) are fitted by the error function (taking into account the analytical results):

$$A\left(1+\mathrm{erf}\left(\frac{\tau-\tau_R}{S}\right)\right). \qquad (1.11)$$

The parameters A, τ_R, S are retrieved from an optimization algorithm (root-mean-square deviations are minimized). A possibility of approximating the leading edge of the part of the waveform reflected from the surface of the reservoir by the error function was proved above within the framework of the theoretical model. Indeed, the exponent in the right-hand side of (1.4) is a smooth function compared to the error function, hence, pulse power rise near the leading edge may be regarded to be specified by the error function. Improved retracking (see fig. 12) gives a better value for the tracking point (the middle of the leading edge of the waveform reflected by water). Only the choice of an adequate optimization technique impedes application of the described method. Note that, when the time of pulse arrival is found by a standard algorithm, the obtained tracking point is in the 32-nd gate of the chart (fig. 12), leading to error in arrival time at 5 gates and in a 2.5 m error in determining water level!

To conclude this section, we formulate the basic principles of the proposed algorithm of regional adaptive retracking, that may be employed for inland as well as for coastal waters:

1) constructing a regional model of reflecting surface (a piecewise constant one);
2) solving a direct problem, modelling waveforms within the model;
3) imposing restrictions and validity criteria for the algorithm on the basis of waveform modelling;
4) solving the inverse problem in two steps: step one – retrieving a tracking point by the threshold algorithm, step two – refinement of the tracking point and (possibly) estimating SWH by solving the optimization problem.

Note that a similar procedure can be used for constructing regional adaptive retracking algorithms for retrieving water level from satellite altimetry for sufficiently complex areas. The surface is divided into fractions with constant parameters (for example, a coastal zone can be represented as 3 strips: sea, land and intermediate area). The contribution of the surface is a sum of contributions from the fractions calculated by the analytical formula (1.4). Then, based on the modelled waveform image the validity criteria are imposed and retracking is improved step-by-step.

4. APPLICATION OF THE ALGORITHM OF REGIONAL ADAPTIVE RETRACKING FOR CALCULATING WATER LEVEL IN THE GORKY RESERVOIR. COMPARISON OF RESULTS OF CACULATION WITH DATA OBSERVED AT WEATHER STATIONS

In this section, the method of adaptive regional retracking, whose theoretical principles were considered above, is employed for water level calculations in the Gorky Reservoir. According to the results presented in Sec. 2 and the criteria of selecting altimetry waveforms, we took for retracking waveforms from the section of the Gorky Reservoir corresponding to 43,14 – 43.22 degrees west longitude. Further, the waveforms were subjected to two-step processing. At the first step, the algorithm of threshold retracking was used, when the arrival

time of the reflected waveform was determined by the power excess over the threshold. The level of the threshold was varied, with data concentration being the best at about 30-50 units of dimensionless power. At the second step (improved threshold), position (the middle of the leading edge of the reflected waveform) of the tracking point was determined more accurately by approximating the leading edge (4 gates near the threshold found at the first step) by the error function (1.11) and minimization of rms deviations.

The results of calculating changes in the water level in the Gorky Reservoir by two-step retracking (dark grey squares) and their comparison with the measurements at the Yurievets weather station (solid line) and GDR base (light grey squares) are presented in fig. 13. The obtained results were used to calculate the correlation coefficient of altimetry data for the 142-nd track of the Jason-1 satellite and data of ground measurements (angular coefficient of the straight lines in fig. 14), and to determine error in assessing water level and amount of valid points in the summer and winter seasons for different retracking algorithms (Table 1). The analysis revealed a significant increase of the number of valid measurement points, as well as a much better correlation between satellite and ground-based data. For example, the correlation coefficient between altimetry data and measurements at the Yurievets weather station increased from 0.33 (with the standard algorithm of high spatial resolution) to 0.88 for the method of adaptive retracking.

5. CONCLUSION

The algorithm for assessing water level in inland water basins and in the coastal zone of the ocean with an error of about 10-15 cm was constructed. The algorithm was tested at the Gorky Reservoir with complex topography, where the standard Ocean-1 algorithm is not applicable resulting in significant data loss. A model of an average waveform reflected from a statistically inhomogeneous piecewise constant surface (topographic model) was constructed. The reflected power was calculated theoretically on the basis of the works by Brown (1977) and Barrick & Lipa (1985). The model was used to substantiate criteria of data selection for the Gorky Reservoir. The water level was calculated by means of regional adaptive retracking of SGDR base for the Gorky Reservoir. It was shown that application of this algorithm greatly increases the number of included data and accuracy of determining water level.

General principles of the proposed algorithm for a complicated area (coastal zone, inland waters, and so on) are based on calculations of the signal with allowance for inhomogeneity of a reflecting surface and may be used in different geographical regions.

6. ACKNOWLEDGEMENTS

The authors thank L. Filina and A. Panyutin for the hydrometeorological data provided. The work was done with financial support from the Russian Foundation for Basic Research (project No. 08-05-97016-r_povolzhye_a).

REFERENCES

AVISO/Altimetry. User Handbook. Merged TOPEX/POSEIDON Products. AVISO. Toulouse. AVI–NT–02–101–CN. Edition **3.0**. 1996. – 201 pp.

ANZENHOFER M., SHUM C.K. and RENTSH M., 1999, Coastal Altimetry and Applications . *Geodetic Science and Surveying*. Tech. Rep. № **464**. The Ohio State University Columbus, USA. 40 pp.

ALSDORF D., BIRKETT C., DUNNE T., MELACK J. and HESS L. 2001. Water level changes in Large Amazon Lake measured with spaceborn radar interferometry and altimetry. *Geophys. Res. Letter* **28**, pp. 2671– 2674. doi: 10.1029/2001GL012962.

BARRICK**,** D. and B. LIPA. 1985, Analysis and interpretation of altimeter sea echo. *Adv. Geophys.* **27**, pp. 61-100.

BROWN G., 1977, The average impulse response of a rough surface and its applications. *Antennas and Propagation, IEEE Trans.* **25**. pp. 67–74. doi: 10.1109/TAP.1977.1141536.

BIRKETT C.M., MERTES L.A.K., DUNNE T., COSTA M.H. and JASINSKI M.J., 2002, Surface water dynamics in the Amazon Basin: Application of satellite radar altimetry. *J. Geophys. Res* **107**, pp. 8059. doi:10.1029/2001JD000609.

BENVENISTE J. and BERRY P., 2004, Monitoring river and lake levels from space. *ESA Bulletin* **117**, pp. 36–42.

BERRY**,** P. A. M., J. D. GARLICK**,** J. A. FREEMAN, and E. L. MATHERS, 2005, Global inland water monitoring from multi-mission altimetry. *Geophysical Research Letters* **32**, L16401, 4 pp., doi:10.1029/2005GL022814

BIRKETT C.M., 1995, The global remote sensing of lakes, wetlands and rivers for hydrological and climate research. *Proc. International Geoscience and Remote Sensing Symposium.. IGARSS '95. Quantitative Remote Sensing for Science and Applications. IEEE. Firenze* **3**, pp. 1979–1981. doi: 10.1109/IGARSS.1995.524084.

BIRKETT C.M., 1998, Contribution of the Topex NASA radar altimeter to the global monitoring of large rivers and wetlands. *Water Resour. Res.* **34,** pp. 1223–1239.

CHELTON, D.B., RIES, J.C., HAINES, B.J., FU, L.-L. and CALLAHAN, P.S., 2001, Satellite Altimetry. In *Satellite Altimetry and the Earth Sciences*: *A Handbook of Techniques and Applications*, Fu, L.-L.& Cazenave A. (Eds.), pp. 1–131 (San Diego CA: Academic Press).

CRETAUX J.-F., CALMANT S., ABARCA DEL RIO R., KOURAEV A., BERGÉ-NGUYEN M., 2010, LAKES studies from satellite altimetry. In *Coastal Altimetry,* S. Vignudelli, A. Kostianoy, P. Cipollini, J. Benveniste. (Eds.) (Berlin, Heidelberg, New York: Springer-Verlag)

CAMPOS I.O., MERCIER F., MAHEU C., COCHENNEAU G., KOSUTH P., BLITZKOW D. and CAZENAVE A., 2001, Temporal variations of river basin waters from Topex/Poseidon satellite altimetry. Application to the Amazon basin. *Earth and Planetary Sciences* **333,** pp. 633-643. doi: 10.1016/S1251-8050(01)01688-3.

DAVIS C. H., 1997, A robust threshold retracking algorithm for measuring ice sheet surface elevation change from satellite radar altimeters. *IEEE Trans. Geosci. Remote Sensing*. **35**, 974-979.

DENG X. and FEATHERSTONE W. E., 2006, A coastal retracking system for satellite radar altimeter waveforms: Application to ERS-2 around Australia. *J. Geophys. Res.* **111,** C06012, doi:10.1029/2005JC003039.

DONELAN M., HAMILTON J. , HUI W. H., 1985, Directional spectra of wind generated waves. *Philos. Trans. Roy. Soc. London, Ser. A*. **315**, pp.509–562.

ENVISAT–ERS, 2004, Exploitation Development of Algorithms for the Exploitation of ERS–ENVISAT Altimetry for the Generation of a River and Lake Product. DMU–RIVL–SPE–03–110. 17 pp.

FRAPPART F., SEYLER F., MARTINEZ J.M., LEON J. and CAZENAVE A., 2005, Floodplain water storage in the Negro River basin estimated from microwave remote sensing of inundation area and water levels. *Remote Sensing of Environment* **99,** pp. 387–399. doi: 10.1016/j.rse.2005.08.016.

FRAPPART F., DO MINH K., L'HERMITTE J., CAZENAVE A., RAMILLIEN G., LE TOAN T. and MOGNARD-CAMPBELL N., 2006, Water volume change in the lower

Mekong from satellite altimetry and imagery data. *Geophys. J. Int*. **167,** pp. 570–584. doi: 10.1111/j.1365-246X.2006.03184.

GLOBE, *Global Land One-km Base Elevation Project*. Available on line at: http://www.ngdc.noaa.gov/mgg/topo/globe.html

KOSTIANOI A.G., ZAVIALOV P.O., LEBEDEV S.A., 2004, What do we know about dead dying and endangered lakes and sea? In *Dying and Dead Seas. Climatic versus Anthropic Causes.,* pp.1-48(Dordrecht.: Kluwer Acad. Publ.)

KOBLINSKY C.J., CLARKE R.T., BRENNER A.C. and FREY H., 1993, Measurement of river level variations with satellite altimetry. *Water Resour. Res.* **29**, pp. 1839–1848. doi: 10.1029/93WR00542.

KOURAEV A.V., ZAKHAROVA E.A., SAMAIN O., MOGNARD N.M. and CAZENAVE A., 2004, Ob' river discharge from TOPEX/Poseidon satellite altimetry (1992-2002). *Remote Sensing of Environment* **93,** pp.238–245. doi: 10.1016/j.rse.2004.07.007.

LEBEDEV S.A. and KOSTIANOI A.G., 2005, *Satellite Altimetry of Caspian Sea.* 366 pp. (Moscow: MORE Publ., Intern. Inst. of the Ocean) (in Russian).

LEE H.K., 2008, Radar altimetry methods for solid earth geodynamics studies. *Geodetic Science and Surveying*. Rep. № **489**., The Ohio State University, 192 pp.

MAHEU C., CAZENAVE A. and MECHOSO C.R., 2003, Water level fluctuations in the Plata Basin (South America) from Topex/Poseidon Satellite Altimetry. *Geophys. Res. Letters.* **30,** pp. 1143–1146. doi: 10.1029/2002GL016033.

MARTIN, T.V.,H.J. ZWALLY,A.C. BRENNER, and R.A. BINDSCHADLER, 1983, Analysis and Retracking of Continental Ice Sheet Radar Altimeter Waveforms, *J. Geophys. Res*.,**88**, pp.1608-1616.

PICOT N., CASE K., DESAI S., VINCENT P., 2008, AVISO and PODAAC User Handbook. IGDR and GDR Jason Products. SMM– MU– M5– OP– 13184– CN (AVISO). JPL D–21352. Edition **4.1**. 130 pp. (PODAAC)

RODRÍGUEZ E. and MARTIN J.M., 1994, Assessment of the TOPEX altimeter performance using waveform retracking. *J. Geophys. Res*. **99**, pp. 24,957–24,969. doi: 10.1029/94JC02030

TOURNADRE J., CHAPRON B., REUL N., and VANDEMARK D. C., 2006, A satellite altimeter model for ocean slick detection. *J. Geophys. Res*., **111**, C04004, doi:10.1029/2005JC003109.

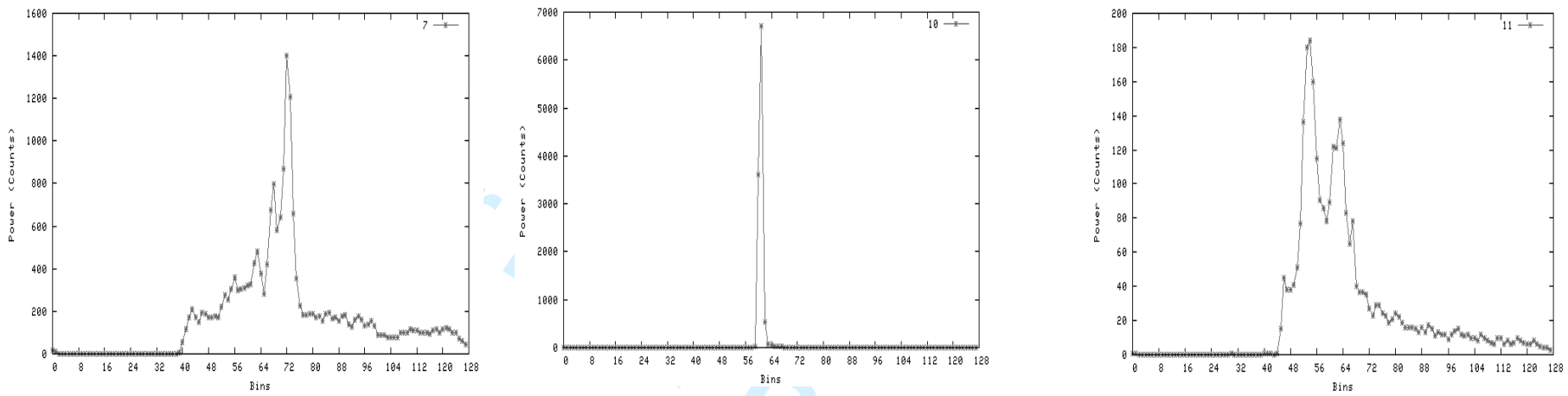

a b c

Figure 1. Waveforms in the coastal zone and inland waters (a) combined reflection from land and water, (b) quasi-specular coherent reflection from a smooth water surface in estuaries and harbors, (c) in the presence of several highly reflecting objects.

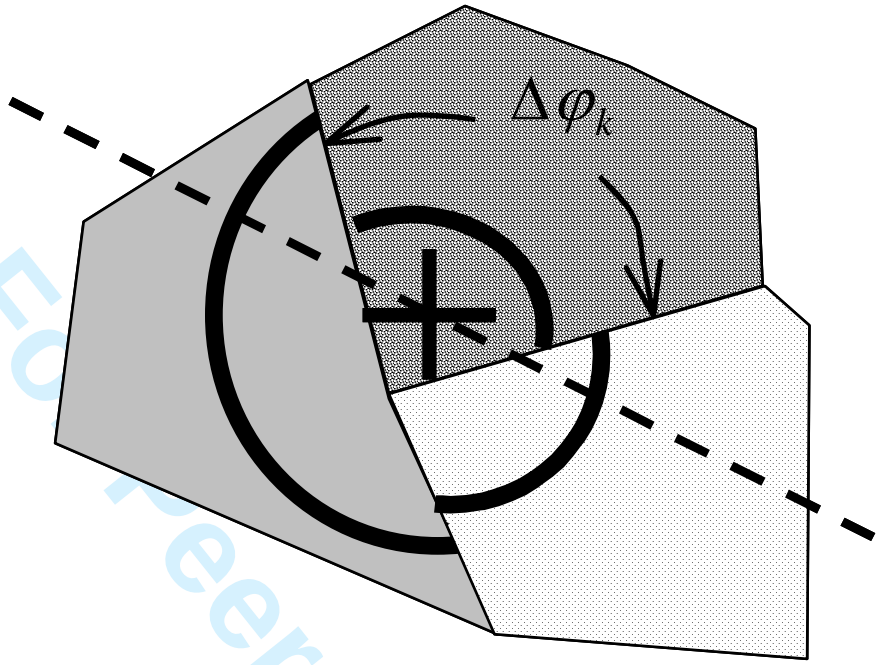

(a)

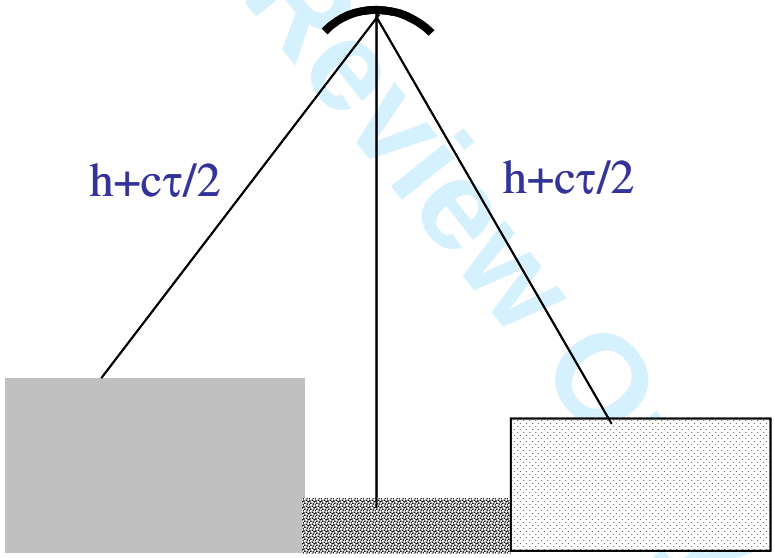

(b)

Figure 2. Piecewise constant model of underlying surface (+ denotes the position of nadir, the dotted line- the track of the satellite, the circle - the border of illuminated area at a given time), a – top view, b – side view.

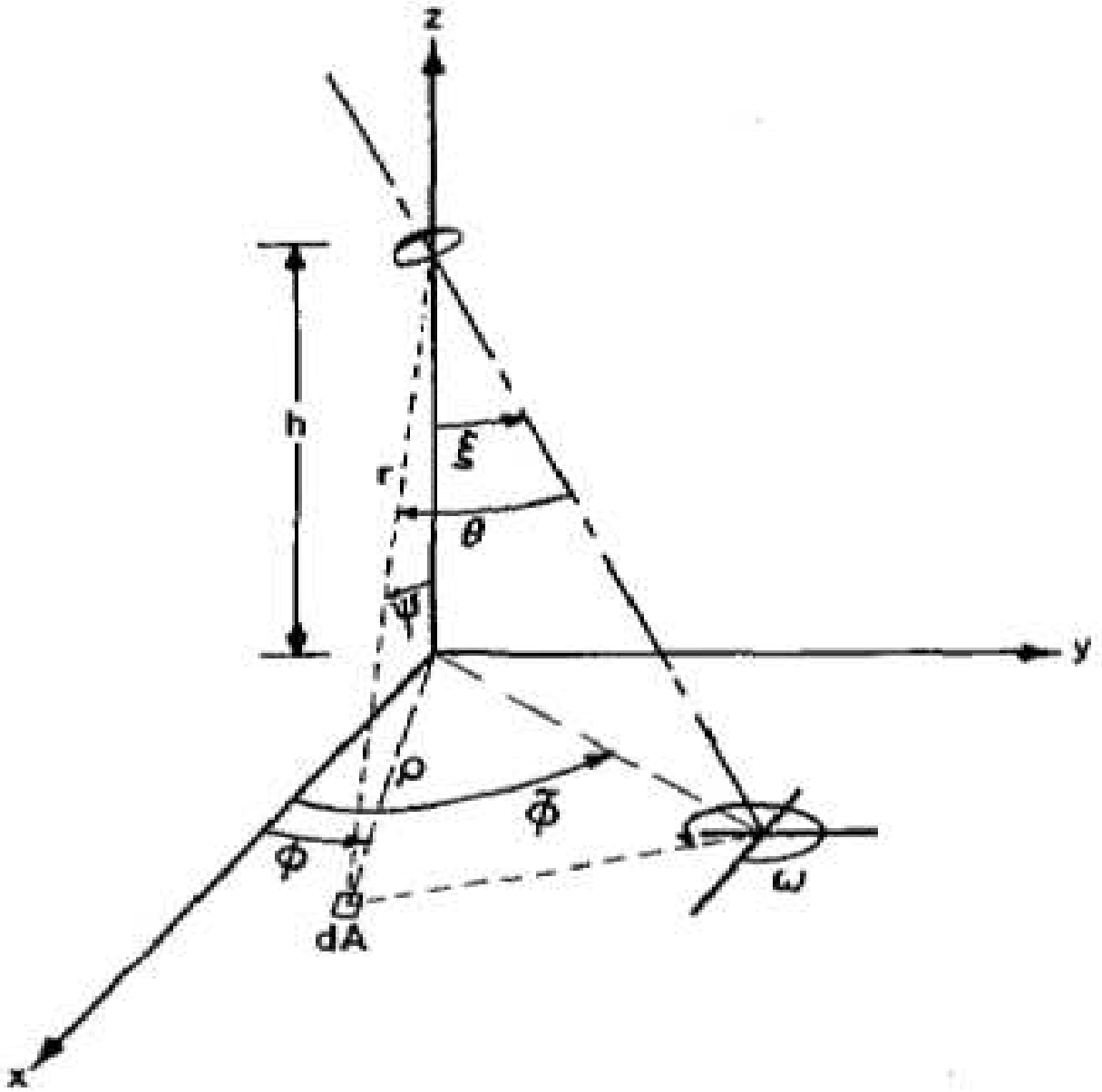

Figure 3. Geometry of the problem (figure reproduced from the paper by Brown, 1977).

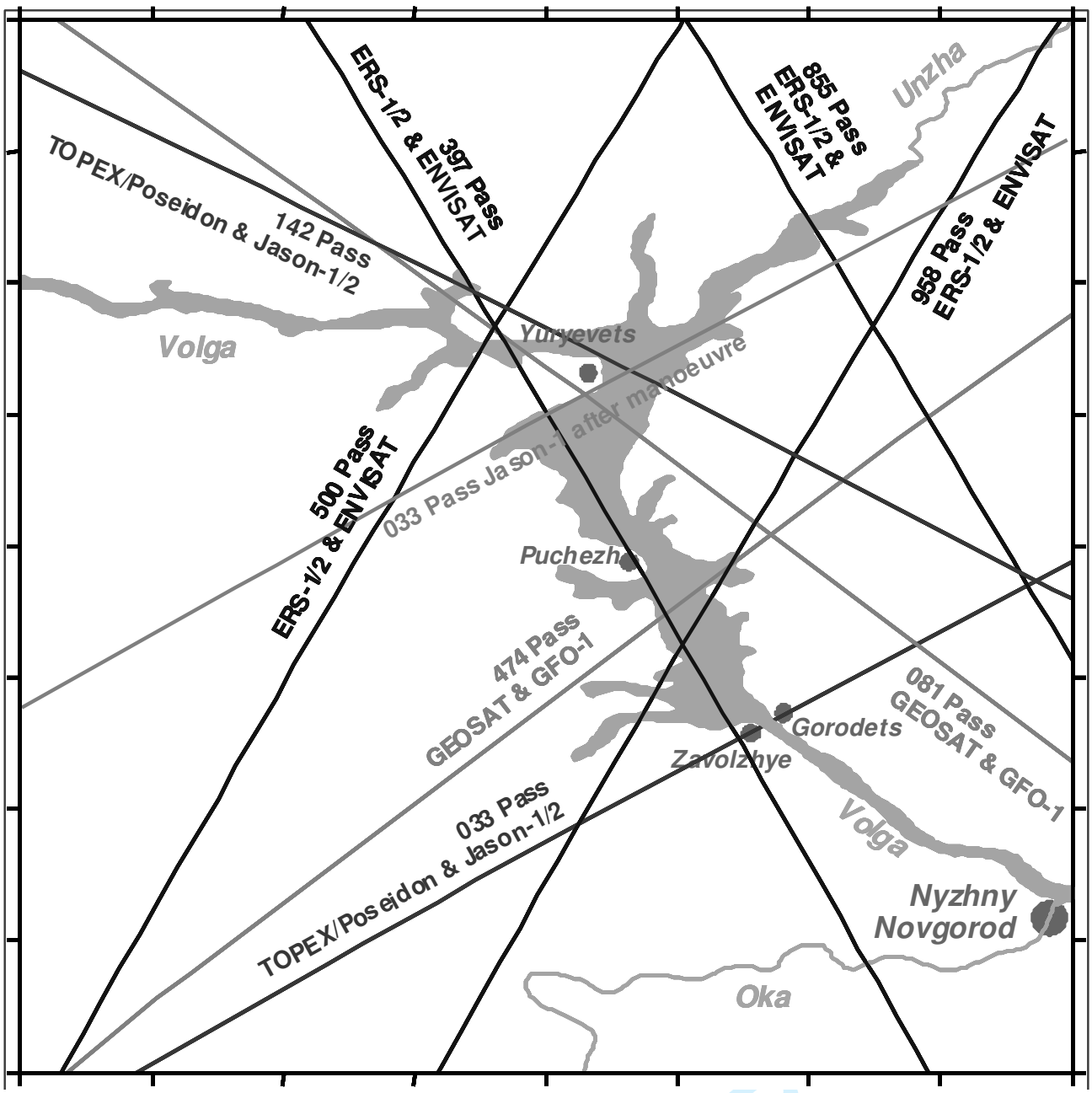

Figure 4. T/P, Jason-1, ERS-1/2, GEOSAT and GFO-1 tracks over the Gorky Reservoir water area.

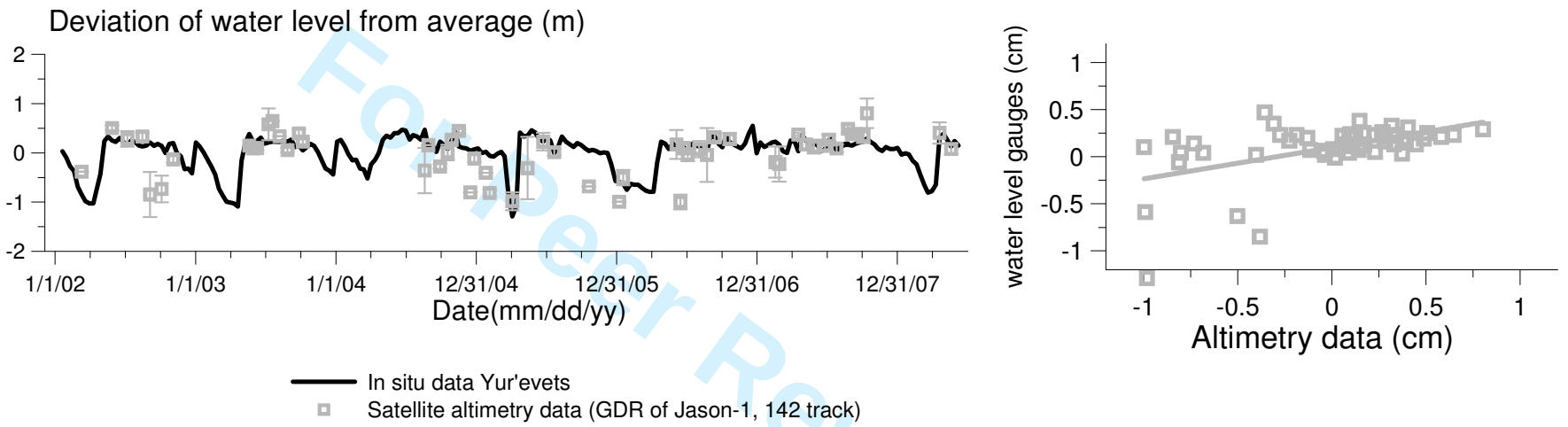

a b

Figure 5. Water level dynamics in the Gorky Reservoir: (a) high-resolution altimetry data for the 142-nd track of T / P and Jason-1 satellites (squares) and meteorological data from Yurievets station (solid line), (b) normalized deviation from the mean water level (squares), best fit (straight line).

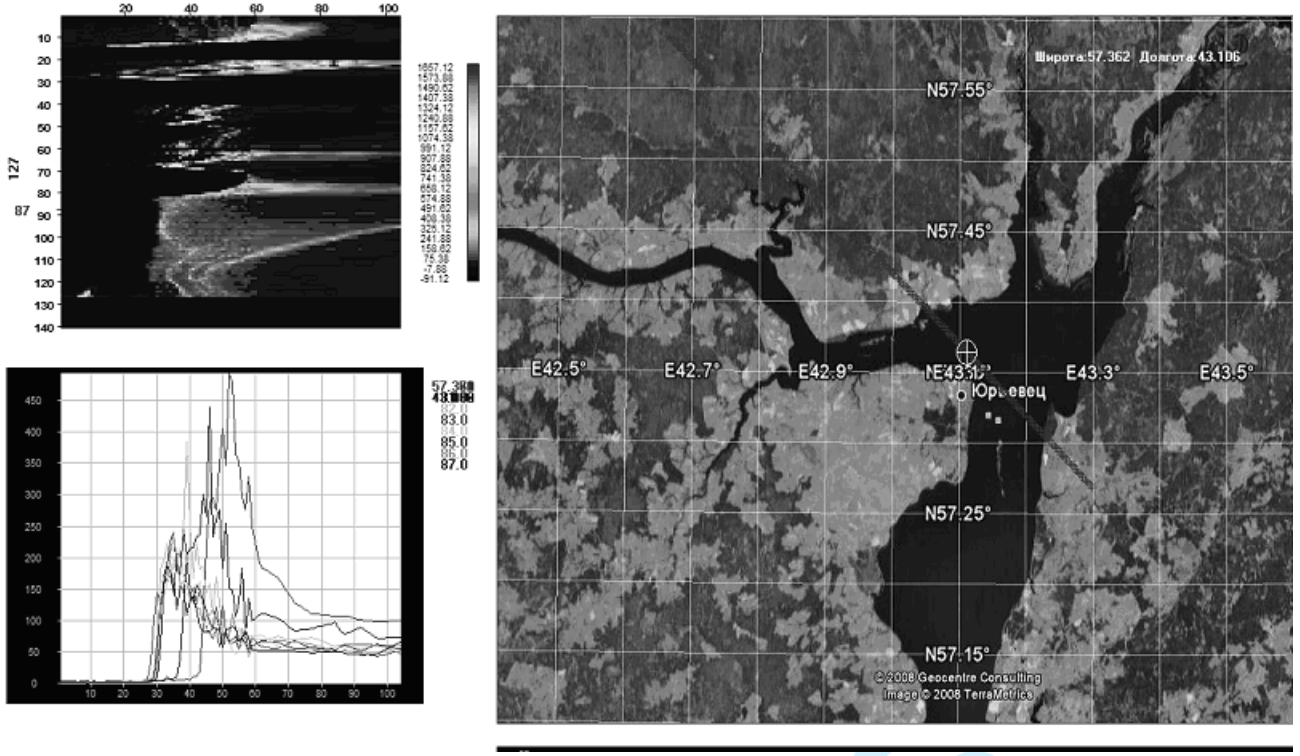

Figure 6. Copy of software monitor with examples of reflected waveforms from SGDR base of Jason-1.

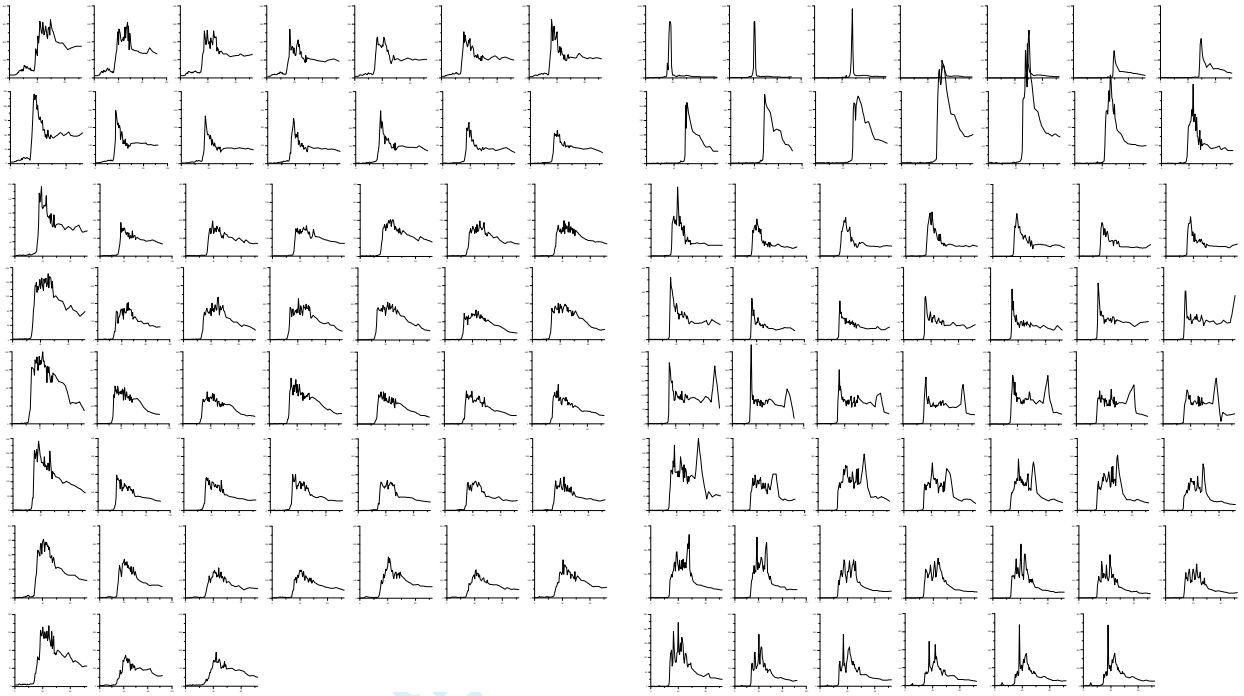

Figure.7. Waveforms of 20-Hz telemetric pulses for 142-nd track of Jason-1 satellite for the Gorky Reservoir: (a) "winter" (03/25/2005), (b) "summer" (05.06.2006).

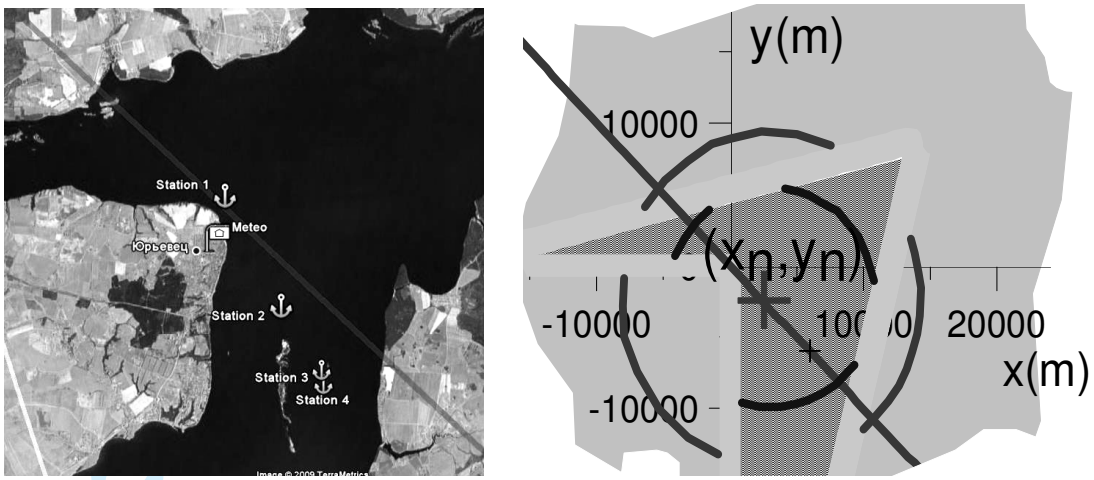

a b

Figure 8. (a) Map of the Gorky Reservoir near the town of Yurievets (straight line – 142-nd track of Jason-1 satellite), (b) piecewise constant model of the underlying surface: dotted shading – water, dark grey – land, light grey – coastal slicks).

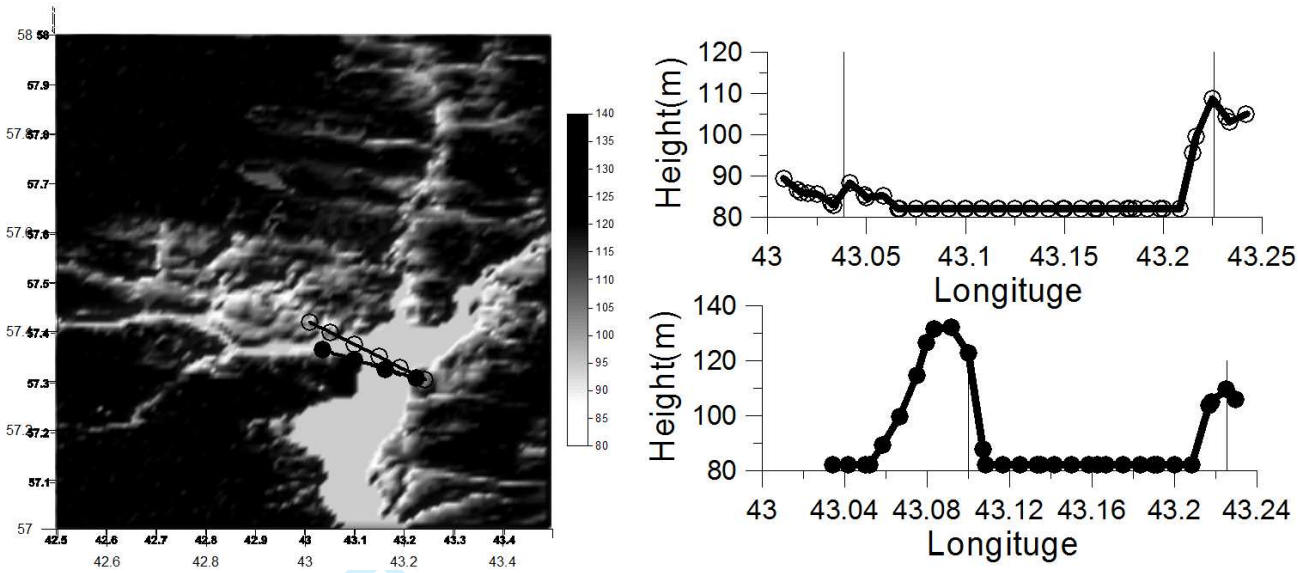

a b

Figure 9. Topology of the surface area near the Gorky Reservoir, taken from the database: http://www.ngdc.noaa.gov/mgg/topo/globe.html (upper right corresponds to the dark grey line on the left panel, bottom right to the light grey line).

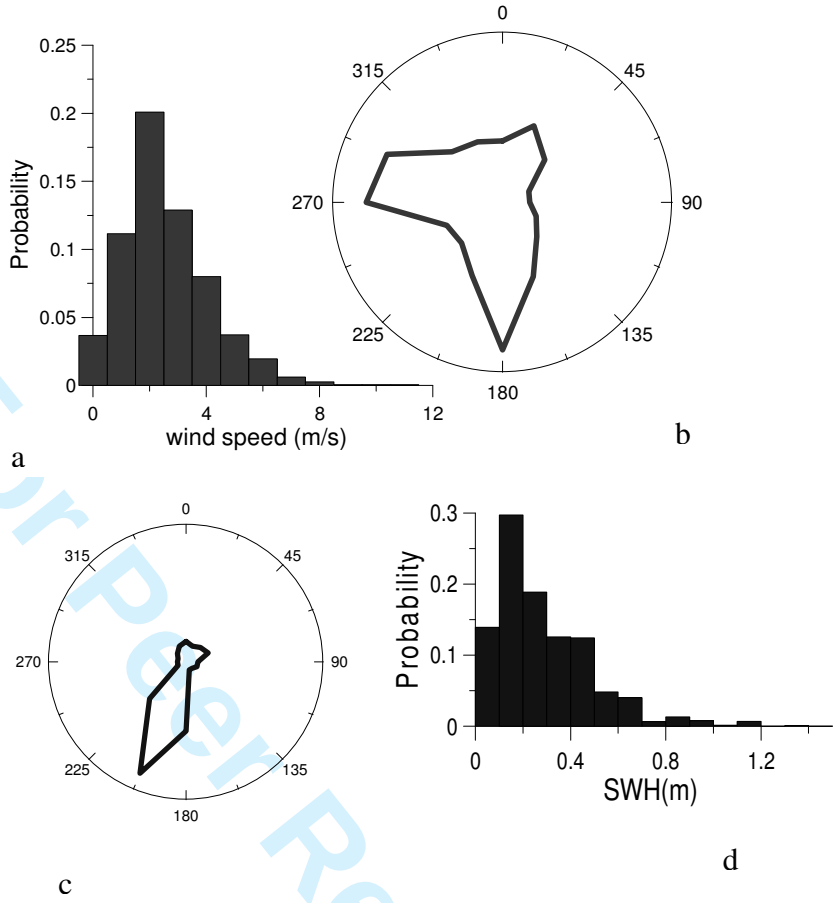

Figure 10. (a) Wind speed and direction in the summer of 2008-2009 (Yurievets weather station, 57 ° 20' .N. 43 ° 07' E), (b) statistics of wind waves (according to field measurements 29/07/2009), (c)-angular distribution of the accelerations for the corresponding wind direction and (d) - histogram of SWH (based on field measurements 29.07.2009) for the mid-point of the track 142 satellite Jason-1.

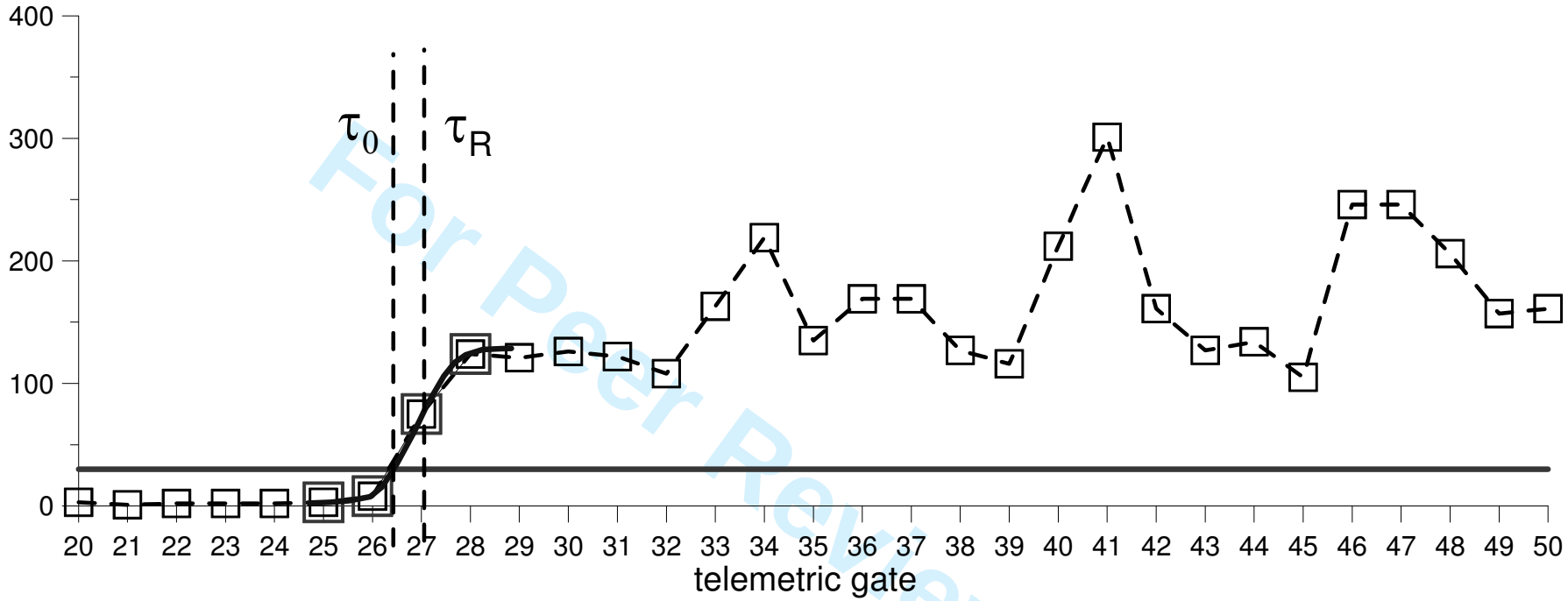

Figure 12. An example of waveform from SGDR of Jason-1, cycle 162, track 142, Ku band (solid line – threshold power, τ_0 – the tracking point for threshold retracking, τ_R – for improved threshold retracking).

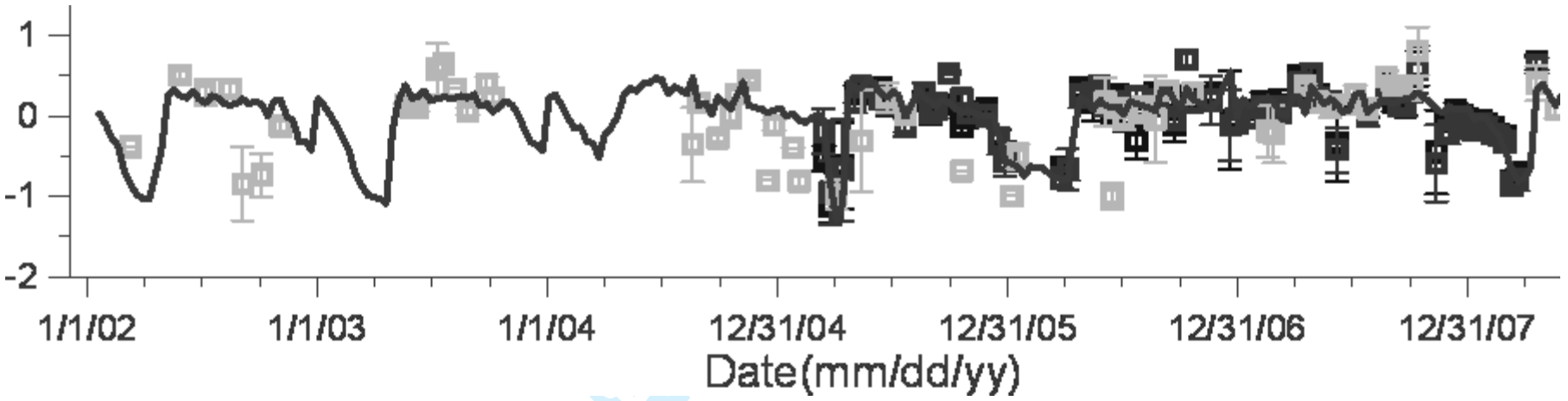

Figure 13. Water level variations in the Gorky Reservoir: GDR high-resolution data for 142 track satellite Jason-1 (open squares), results of retracking SGDR base from Jason-1 satellite (filled squares) and meteorological data from Yurievets (solid line).

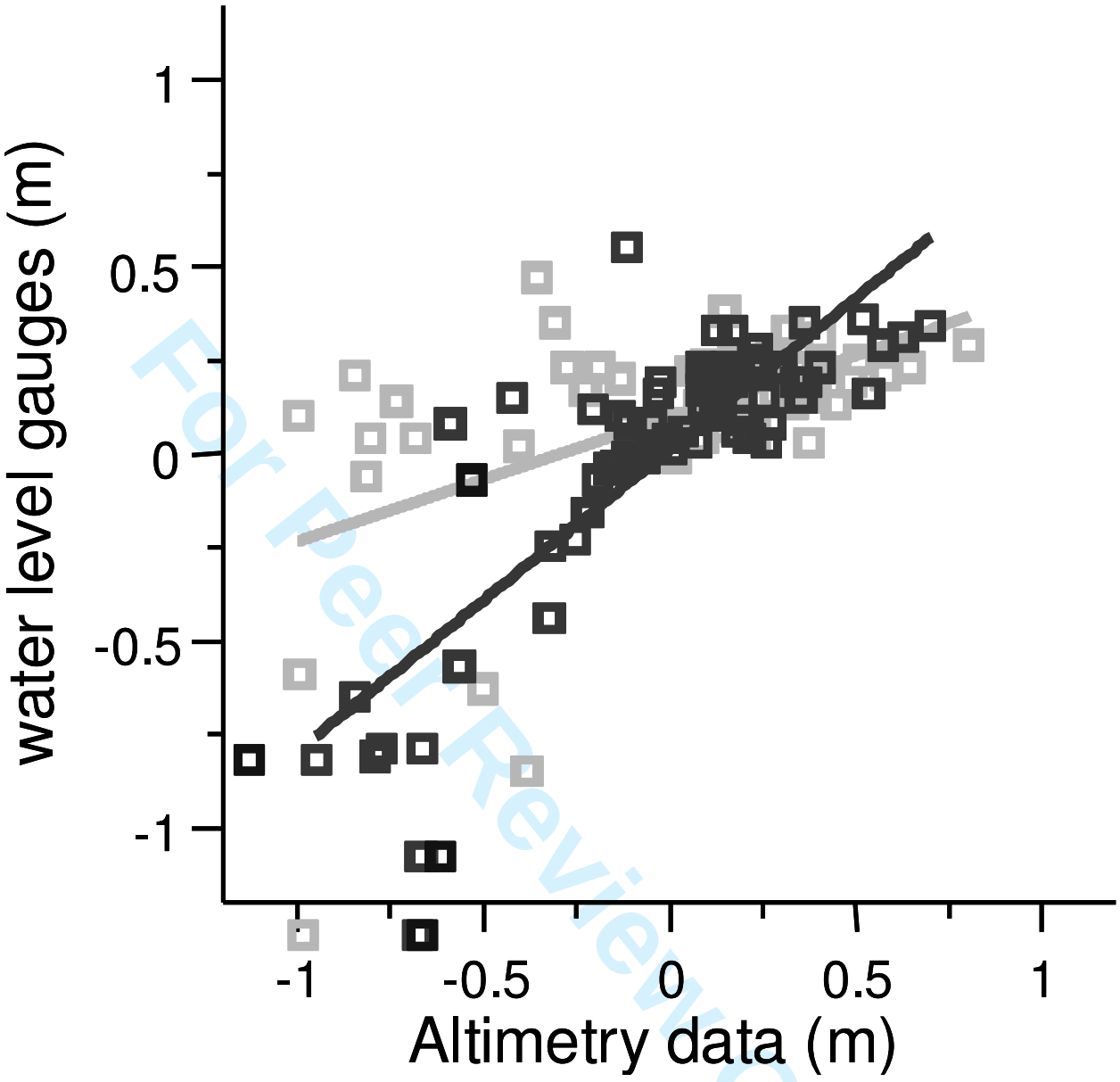

Figure14. Normalized deviation from mean water level: GDR base – light grey squares, results of retracking SGDR base – dark grey squares. Best fit lines: light grey and dark grey, respectively.

Table 1. Standard deviation of the water level in the Gorky Reservoir and average number of valid points per month (for SGDR base regional retracking for 142-nd track of Jason-1).

	Standard deviation of the water level (m)		Average number of valid points per month	
Method of retracking	Winter (November-April)	Summer (May – October)	Winter (November-April)	Summer (May – October)
GDR data	0.15	0.16	0.3	1.2
Retracking by the threshold method	0.15	0.13	1.5	2.0
Retracking by the improved threshold method	0.18	0.12	1.5	2.0